Audio Engineering Society

Convention Paper 10416

Presented at the 149th Convention
Online, 2020 October 27-30

Estimating Nonlinear Impulse Response Length using Time-Delayed Mutual Information

Ethan R. Hoerr[1] and Robert C. Maher[1]

[1]*Electrical and Computer Engineering, Montana State University, Bozeman, MT USA 59717-3780*

Correspondence should be addressed to Ethan Hoerr (ethan.hoerr@student.montana.edu)

ABSTRACT

Using impulse responses measured from various audio systems has become common in audio signal processing. However, determining the length of an impulse response captured from a nonlinear system becomes problematic, as these systems violate the linearity principle from signals and systems theory. A "lumpy" or "spiky" tail in the measured impulse response of a nonlinear system is a tell-tale symptom of this issue. In this in-progress work, we investigate the use of time-delayed mutual information (TDMI), a concept from the field of information theory, to identify the useful portion of a recovered nonlinear impulse response. Initial test systems include linear, time-invariant FIR and IIR filters, and IIR filters with a static nonlinear distortion added.

1 Introduction

The problem of noise contaminating the recovered impulse response of a system with nonlinearities is well-known [1, 2, 3] Often, this noise will manifest as a "lumpy" tail in the impulse response. This phenomenon can complicate the issue of determining the actual length of the impulse response. When using the measured response for filtering audio signals, excluding as much of the noise improves distortion immunity [3]. In recent work, truncating the measured Volterra kernels of tube amplifiers improved model performance and reduced computational complexity [4].

This in-progress work investigates estimating the memory length of nonlinear systems using time-delayed mutual information (TDMI), a technique originating from the information theory field [5]. TDMI is not a modeling technique, rather, it is a method to quantify the nonlinear correlation between two signals across various time-shifts [6]. In this case, the two signals are the input and output of a nonlinear system, and the TDMI should indicate the memory extent or impulse response length of the system. Thus, we hope to demonstrate that TDMI can help distinguish a nonlinear system's recovered impulse response from noise due to nonlinearities.

To evaluate how well this technique estimates a system's memory length, we first apply it to linear, time-invariant FIR and IIR filters to develop confidence in applying the same method to nonlinear systems. We evaluate the TDMI performance by comparing the results to the expected impulse response length. By establishing a strong foundation on known systems, we can then address known nonlinear systems with con-

fidence, and eventually, unknown systems that may exhibit nonlinear behavior.

2 Background: Time-Delayed Mutual Information

Mutual information measures the reduction in uncertainty about the probability of a random process X given information from another process Y [5]. In an audio signal processing context, the processes X and Y can be the sampled input and output signals $x[n]$ and $y[n]$ of an audio system. Mutual information principally requires estimating the marginal and joint probabilities of X and Y; that is, $P(X)$, $P(Y)$, and $P(X,Y)$. In this work, we use the histogram as our estimator, as it performs satisfactorily for the length of signals we will be using [6]. Next, the Shannon entropy of each of these probabilities is computed, using

$$H_X = -\sum_i p(x)\log_2 p(x) \text{ bits/symbol} \quad (1)$$

$$H_Y = -\sum_i p(y)\log_2 p(y) \text{ bits/symbol} \quad (2)$$

$$H_{X,Y} = -\sum_i p(x,y)\log_2 p(x,y) \text{ bits/symbol} \quad (3)$$

With the entropies of each probability distribution computed, the mutual information (MI) is given by the sum of the marginal entropies minus the joint entropy [5]:

$$MI = H_X + H_Y - H_{X,Y} \quad (4)$$

If the input and output signals are statistically independent – that is, $p(x,y) = p(x)p(y)$ – the mutual information between the two will be 0. Conversely, significant mutual information values are indicated where they are greater than the estimator bias or "noise floor" of the probability estimator; determining this estimator bias will be covered shortly. Now, introducing a time-shift τ in one of the random processes gives the time-delayed mutual information (TDMI):

$$MI(\tau) = H_{X(\tau)} + H_Y - H_{X(\tau),Y} \quad (5)$$

By evaluating the TDMI in Equation 5 over a series of time-shifts τ, we estimate the impulse response length by counting how many samples it takes until the TDMI values fall into the estimator bias or "noise floor". To find the estimator bias, we first apply a random shuffle algorithm to the input signal $x[n]$, reordering the sequence elements randomly. Then, for each time shift τ applied to the shuffled $x[n]$, we measure the mutual information between $x[n-\tau]$ and the unaltered output signal $y[n]$ [6]. Theoretically, there should be no mutual information between these signals; TDMI values less than or equal to this estimator bias shall be deemed insignificant.

3 Experiment

3.1 Test Script Setup

The following parameters are common to all of the TDMI experiments that follow. Based on the cross-correlation method used in [4] and [7], we use the MATLAB function `randn` to generate the test system's input signal $x[n]$, creating a pseudo-random Gaussian white noise sequence of sample length $N^2 = 10^6$, where the histogram bin count $N = 10^3$. $x[n]$ is then passed through the test system and the output signal is recorded as $y[n]$. Using N bins, the marginal probabilities $P(X)$ and $P(Y)$ and the joint probability $P(X,Y)$ are computed with the `histogram` and `histogram2` MATLAB functions, respectively. Finally, the user must specify an array of sample-shifts τ over which to compute the TDMI.

Once the signals $x[n]$, $y[n]$, the bin count N, and the array of sample-shifts τ are decided, they are passed into a custom MATLAB function, `tdmi`. This function iterates over all sample-shifts τ provided, finding each probability distribution and its associated Shannon entropy, as given in Equations 1-3. Then, the function computes the TDMI for each sample shift τ as shown in Equation 5. For each value τ, the function also determines the estimator bias as described in the previous section. The function then returns the sample-shifts, TDMI values, and estimator bias as separate arrays for analysis and plotting.

In the sections that follow, we start with relatively simple test systems for evaluating the TDMI method, including a delay line and FIR moving average filter. Then, we look at IIR lowpass filters, briefly discuss all-pass filters with various levels of attenuation, and finally, we examine the same IIR filters but with a nonlinear distortion added to the filter output.

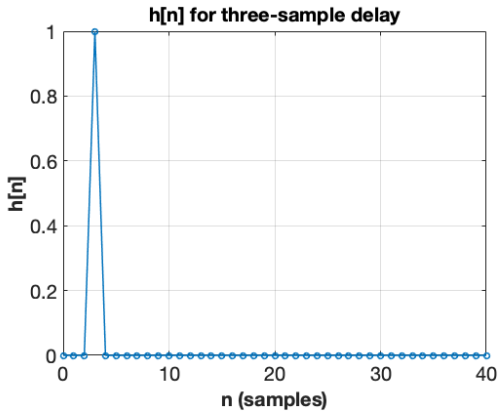

Fig. 1: Impulse response of delay system described in Eq. 6

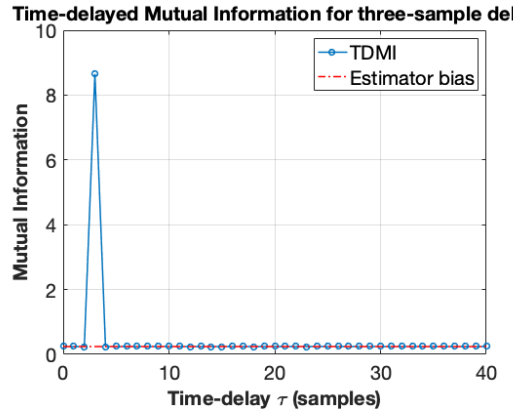

Fig. 2: TDMI evaluated over $\tau = [0, 40]$ for delay system described in Eq. 6

3.2 First experiment: Simple delay system

As a straightforward first demonstration, our initial test system is simply a delay of three samples:

$$h[n] = \delta[n-3] \tag{6}$$

The impulse response for Equation 6 be seen in Figure 1. After passing the input signal $x[n]$ through the system and recording the output $y[n]$, we then compute the TDMI and estimator bias over sample-shifts ranging from zero samples to 40 samples; see Figure 2.

Here we once again emphasize that the computed TDMI values do not serve as a model of the test system, but as an estimate of the impulse response length. The singular spike in TDMI corresponds to where the most mutual information between $x[n]$ and $y[n]$ occurs. Because $y[n]$ is simply a copy of $x[n]$ delayed by three samples, the maximum TDMI between $y[n]$ and x[n] occurs at $\tau = 3$, where $x[n]$ is delayed by three samples. In contrast, the TDMI values at any other time-shift τ are indistinguishable from the estimator bias or TDMI "noise floor".

3.3 Second experiment: FIR Moving Average filter

To further evaluate TDMI as a method for estimating impulse response length, we cascade the three-sample delay with a moving-average FIR filter containing 10 coefficients of $\frac{1}{10}$ each, resulting in the following impulse response:

$$h(n) = \begin{cases} \frac{1}{10}, & 3 \leq n \leq 12 \\ 0, & \text{otherwise} \end{cases} \tag{7}$$

The impulse response for this system is shown in Figure 3; evaluating the TDMI across sample-shifts from $\tau = 0$ to $\tau = 40$ is shown in Figure 4. In this example, the TDMI is clearly above the estimator bias for the active part of the filter, where $3 \leq \tau \leq 12$ sample-shifts. Thus, while we do not create a model of the test system using TDMI, we can confidently estimate the length of its impulse response.

3.4 Third experiment: IIR filters

With the basic examples of a delay line and a basic FIR filter validated, the next degree of complexity is to consider systems characterized by an infinite impulse response (IIR). Due to the analog nature of audio systems like amplifiers and filters, we must expect to encounter such IIR systems in the "real world". Hence, in this experiment, we investigate the performance of the TDMI approach on RC low-pass filters digitized using the impulse invariance method. Because RC low-pass filters are well understood and easy to design, we chose to focus on their digitized versions as our first IIR test systems. Despite the fact that the impulse response length of these filters is truly infinite, a common heuristic states that the impulse response decays after five

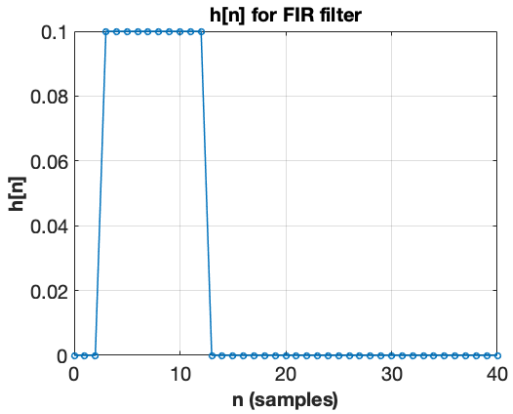

Fig. 3: Impulse response of delayed, FIR moving-average system described in Eq. 7

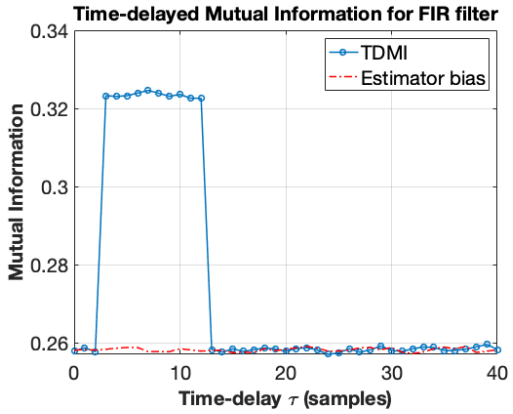

Fig. 4: TDMI evaluated over $\tau = [0,40]$ for delayed, FIR moving-average system described in Eq. 7

time constants. Therefore, this rule of thumb will be useful when interpreting the calculated TDMI values.

To conduct the following IIR experiments, using the impulse invariance method, we designed RC lowpass filter prototypes with various cutoff frequencies of f_c =1, 2, 5, 10, and 20 kHz, using a sampling frequency of $f_s = 96$ kHz. The Laplace-domain transfer function for the RC filters is given by

$$H(s) = \frac{2\pi f_c}{s + 2\pi f_c}, \tag{8}$$

where $2\pi f_c = \frac{1}{RC}$. We obtain the discrete-time RC filters using the impulse invariance relation from [8],

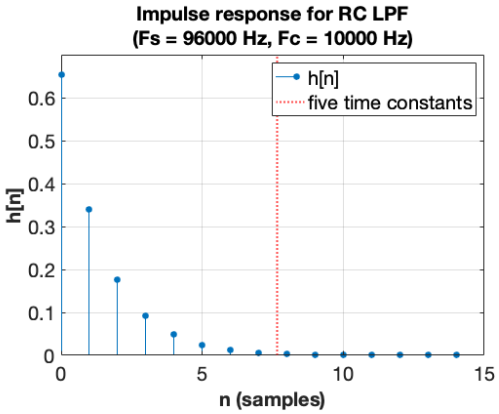

Fig. 5: Impulse response for digitized RC Lowpass Filter with $f_c = 10$kHz

$$H(z) = \frac{2\pi f_c t_0}{1 - e^{-2\pi f_c t_0} z^{-1}}, \tag{9}$$

where $t_0 = 1/F_s$, for $F_s = 96$kHz. To evaluate the TDMI method for our lowpass filter prototypes, we apply the same method as before: pass pseudo-random Gaussian white noise through the system defined by $h[n]$, select sample-shifts τ over which to evaluate the TDMI, and pass $x[n]$, $y[n]$, and the lags into our MATLAB function `tdmi`.

3.4.1 10kHz low-pass IIR filter

Starting with $f_c = 10$kHz, the impulse response of the designed low-pass filter is shown in Figure 5. The abscissa is shown in samples based on F_s. Although five time constants in continuous-time does not correspond to an integer number of samples, it is nonetheless plotted as a vertical line for reference. Figure 6 shows the TDMI calculation and estimator bias for the filter with $f_c = 10$kHz.

Also in the TDMI calculation shown in Fig. 6, we plot five time constants as a vertical dotted line for reference. In addition, we indicate where the TDMI is less than or equal to the estimator bias with a star. As seen in Fig. 6, the significant portion of the TDMI occurs between $0 \leq n \leq 6$. With this particular filter, five time constants multiplied by F_s corresponds to 7.6394 samples. Hence, we have some confidence that the TDMI could estimate the length of the impulse response for $h[n]$ in this instance.

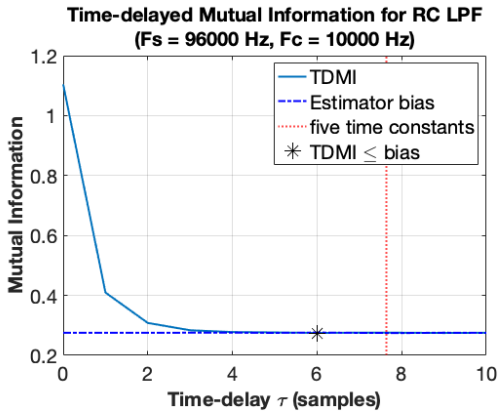

Fig. 6: TDMI evaluated for RC Lowpass Filter with $f_c = 10$kHz

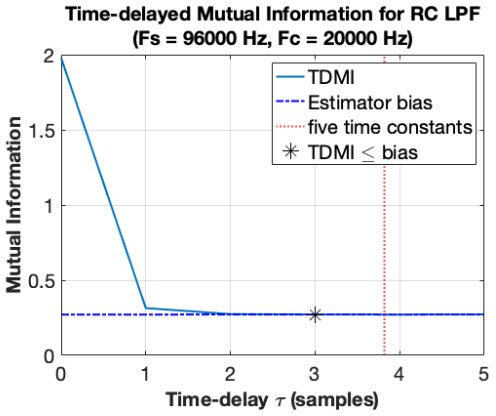

Fig. 8: TDMI evaluated for RC Lowpass Filter with $f_c = 20$kHz

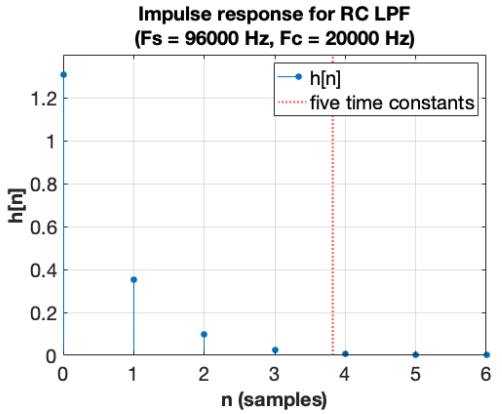

Fig. 7: Impulse response for digitized RC Lowpass Filter with $f_c = 20$kHz

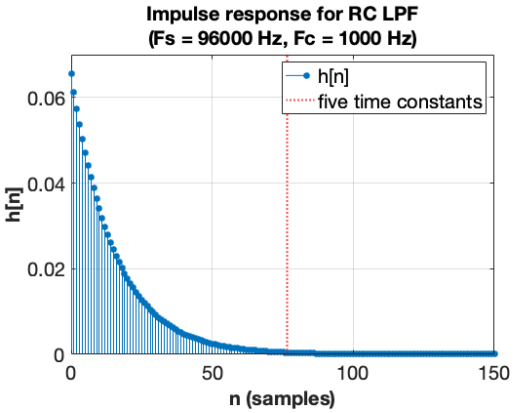

Fig. 9: Impulse response for digitized RC Lowpass Filter with $f_c = 1$kHz

3.4.2 20kHz low-pass IIR filter

Next, we look at the case where $f_c = 20$kHz. Its impulse response and TDMI plot are shown in Figures 7 and 8, respectively. The results are similar to the $f_c = 10$kHz case: the TDMI is above the estimator bias between $0 \leq \tau \leq 3$ sample-shifts, slightly short of the five time constants mark of 3.8197 samples when scaled by $F_s = 96$kHz. Thus, while the TDMI method did not perfectly predict the impulse response length, it seemed to perform relatively well.

3.4.3 1, 2, and 5kHz low-pass IIR filters

We noticed an interesting phenomenon when dealing with low-pass filters with narrower passbands. In this subsection, we examine the TDMI method as applied to filters with cutoff frequencies of 1, 2, and 5 kHz, respectively. The impulse response plots and TDMI calculations for these three filters are shown in Figures 9 through 14.

We can see that as the passband shrinks by reducing f_c, the TDMI approach gets worse at predicting the impulse response length. In the 1kHz example, the TDMI falls below the estimator bias for $\tau \geq 35$ samples, yet

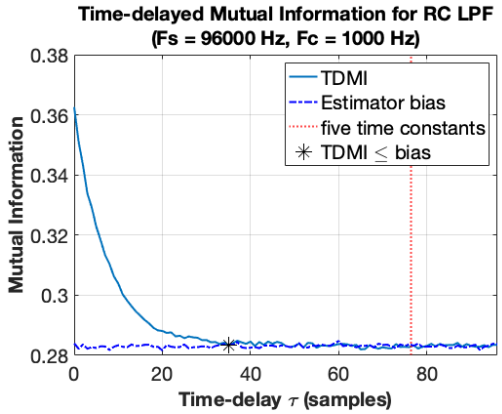

Fig. 10: TDMI evaluated for RC Lowpass Filter with $f_c = 1$kHz

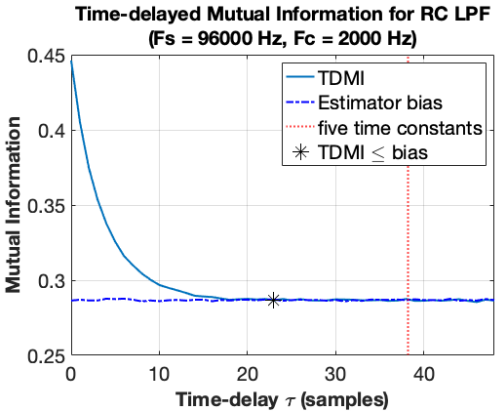

Fig. 12: TDMI evaluated for RC Lowpass Filter with $f_c = 2$kHz

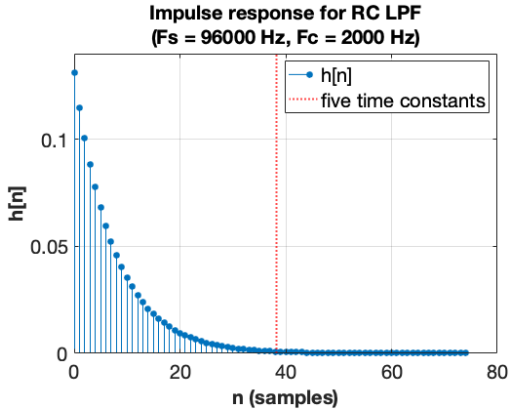

Fig. 11: Impulse response for digitized RC Lowpass Filter with $f_c = 2$kHz

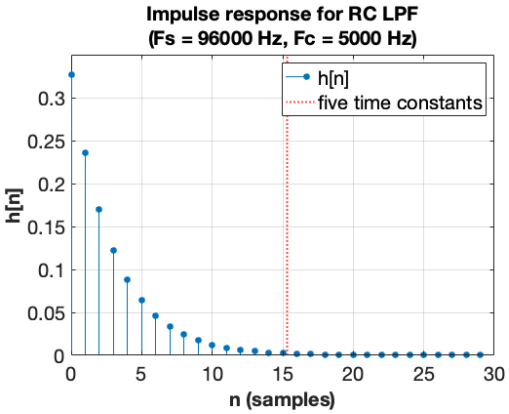

Fig. 13: Impulse response for digitized RC Lowpass Filter with $f_c = 5$kHz

the scaled five time constants occurs at 76.3944 samples. In the 2kHz example, the TDMI method indicates significant values between $0 \leq \tau \leq 34$, while the scaled five time constants should be 38.1972 samples. Thus, the TDMI already seems to improve compared to the 1kHz case. Finally, for $f_c = 5$kHz, TDMI is significant for $0 \leq \tau \leq 14$, and five time constants occurs at 15.2789 samples.

At the time of this preprint, we are still investigating the cause of this phenomenon. Initially, it appears that the power of the filtered output signal $y[n]$ shrinks as we reduce the filter cutoff frequency, f_c. Intuitively, this is no surprise as the filter blocks certain frequencies of the broadband noise in the test signal $x[n]$. To check whether the decreased power of the output signal was causing this phenomenon, in the next section we present tests using all-pass filters with gradually decreasing gains.

3.5 All-pass filters with decreasing gains

As mentioned in the previous subsection, the TDMI method when applied to lowpass filters becomes unreliable as the pass band becomes narrower. As part of the initial investigation into this observation, here we present the TDMI method applied to Schroeder all-pass filters with various levels of attenuation. In doing so, we hope to verify whether the reduction in the level of

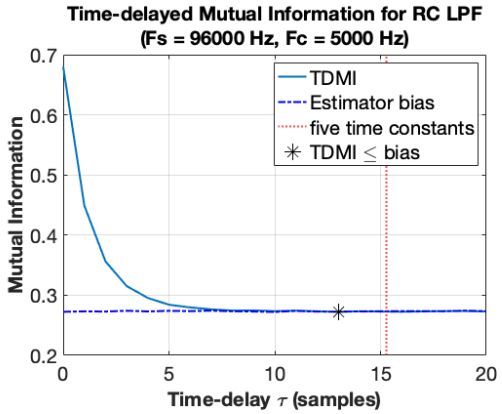

Fig. 14: TDMI evaluated for RC Lowpass Filter with $f_c = 5$kHz

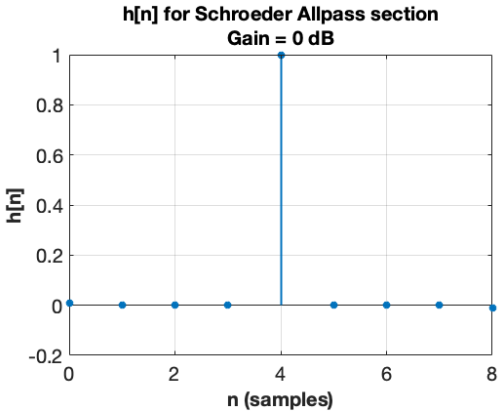

Fig. 15: Impulse response for all-pass filter with 0dB of attenuation

output signal $y[n]$ is attributable to the unreliable TDMI values.

From [9] we use the following discrete-time transfer function to create Schroeder all-pass filter sections:

$$H(z) = \frac{b_0 + z^{-M}}{1 + a_M z^{-M}}, \tag{10}$$

where we arbitrarily set the delay line length to $M = 4$ samples and set the feedback and feedforward coefficients $b_0 = a_M = 0.01$. We scale $H(z)$ in Eq. 10 by the constants 1, 2^{-10}, and 2^{-20} to apply varying amounts of attenuation to the system. These scalars correspond to 0, -60, and -120 dB of gain, respectively. The resulting impulse response and TDMI results for an all-pass filter with unity gain are given in Figures 15 and 16, respectively. The TDMI calculation for an all-pass filter with -120 dB gain is shown for comparison in Figure 17. We did not show figures for the -60 dB case because, regardless of the attenuation we applied to the all-pass filter, the TDMI calculation always indicated that the significant portion of the impulse response occured at $\tau = 4$ samples, which corresponds to the impulse response peak as shown in Figure 15. Thus, we cannot say that merely reducing the amplitude of $y[n]$ will produce unreliable TDMI estimations, and we will need to address the issue in the previous section as future work.

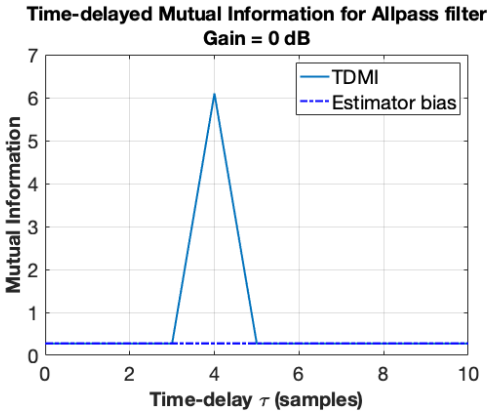

Fig. 16: TDMI evaluated for all-pass filter with 0dB of attenuation

3.6 IIR Lowpass filters with static nonlinearity

Finally, we look at the TDMI method when applying a static nonlinearity to the output of the lowpass filters designed in Section 3.4. As in our prior work [7], we use the arctangent function to serve as a "soft-clipping" static nonlinearity. This function is shown in Figure 18. TDMI plots for the 1, 2, 5, 10, and 20 kHz lowpass filters with added nonlinear distortion are shown in Figures 19 through 23.

Comparing the distorted filters with their linear counterparts, the TDMI calculations included more of the impulse response length for the 1kHz case, and underestimated the impulse response length for the 2kHz,

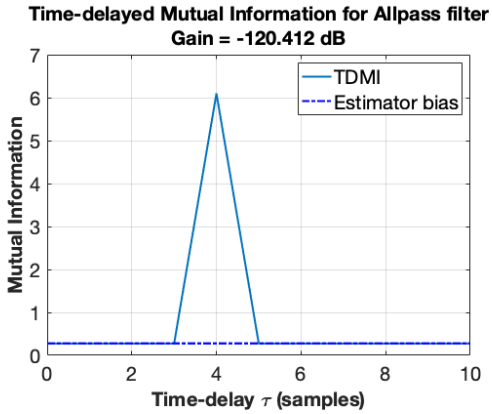

Fig. 17: TDMI evaluated for all-pass filter with 120dB of attenuation

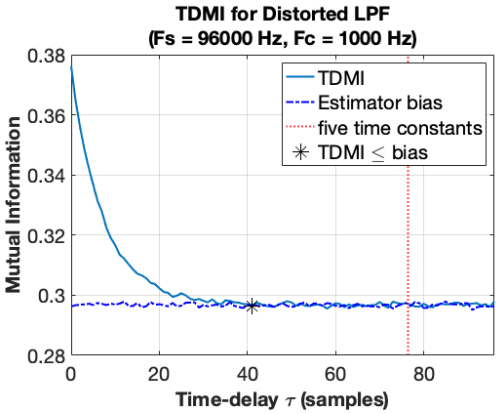

Fig. 19: TDMI evaluated for Distorted RC Lowpass Filter with $f_c = 1$kHz

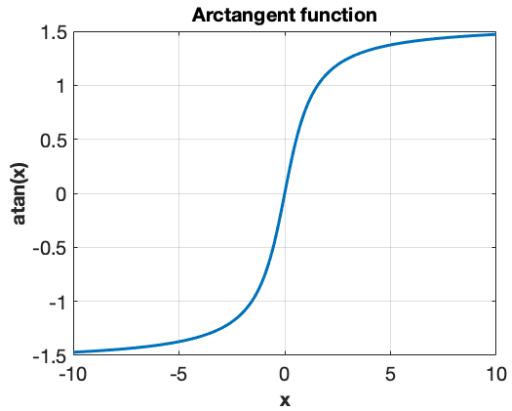

Fig. 18: Arctangent function evaluated over $-10 \leq x \leq 10$

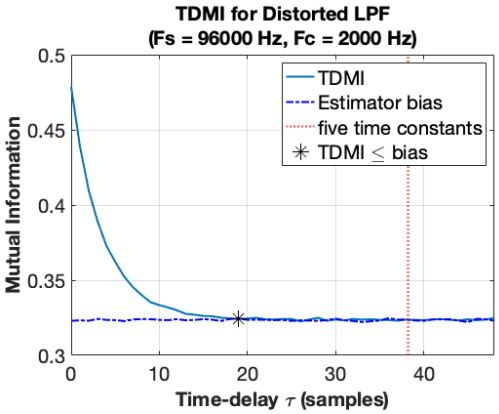

Fig. 20: TDMI evaluated for Distorted RC Lowpass Filter with $f_c = 2$kHz

5kHz, and 10kHz cases. The nonlinear 20kHz case appeared to perform similarly to the linear case, as it overestimated the impulse response length by about 1 sample. However, the linear 20kHz case underestimated the length by 1 sample. We did not observe the same trend in the linear experiments, where TDMI was less reliable as f_c decreased.

4 Discussion

For fairly simple scenarios such as a delay line (Eq. 6), FIR moving-average filter (Eq. 7), and various Schroeder all-pass filters (Eq. 10), the TDMI method accurately reported the significant portion of the system's impulse response. Once we shifted our focus to IIR lowpass filters (Eq. 9), we noticed that the performance of the TDMI method worked for fairly generous passbands, but started to degrade as f_c was decreased. When adding the arctangent as a nonlinear distortion to these linear filters, the TDMI did worse for larger f_c but actually did better for $f_c = 1$kHz. There did not seem to be much difference between the linear and nonlinear 20kHz lowpass filter experiment. In the former, the impulse response length was underestimated by 1 sample, while in the latter, the length was overestimated by the same amount.

Future work includes investigating the degradation of the TDMI method as f_c decreases in the linear case. We initially thought that the TDMI method might suf-

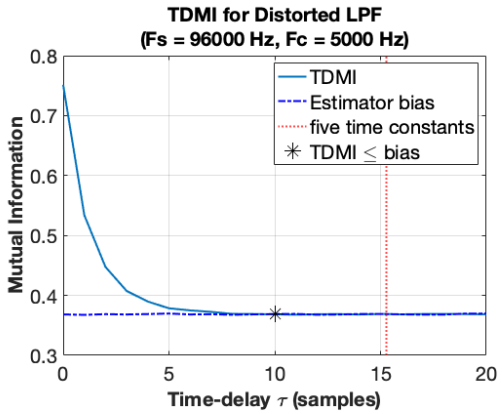

Fig. 21: TDMI evaluated for Distorted RC Lowpass Filter with $f_c = 5$kHz

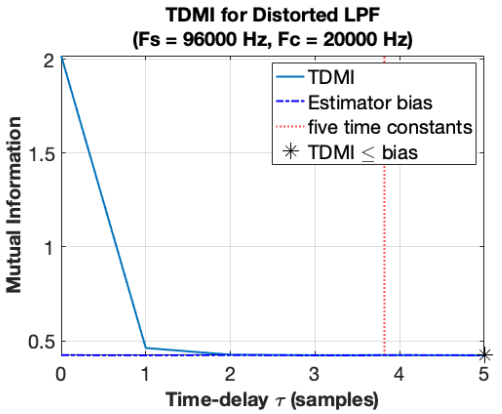

Fig. 23: TDMI evaluated for Distorted RC Lowpass Filter with $f_c = 20$kHz

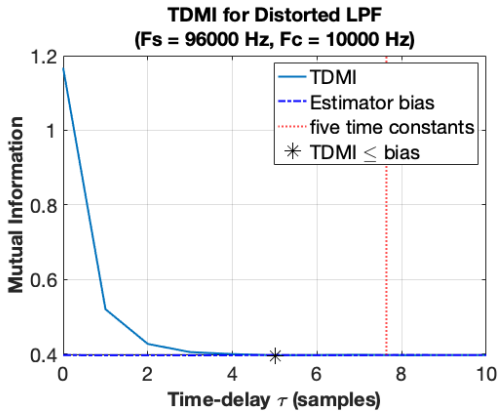

Fig. 22: TDMI evaluated for Distorted RC Lowpass Filter with $f_c = 10$kHz

fer if the amplitude of the output becomes extremely small, but the method worked perfectly on an all-pass filter with -120dB gain. Importantly, the TDMI calculations are dependent on the estimated probability distributions for the input and output signals. Thus, the next logical step is to investigate these distributions more closely as f_c varies. When adding the nonlinear distortion, the TDMI approach generally seemed to underestimate the impulse response length compared to the undistorted experiments. Again, investigating the calculated probability distributions in these cases will be worthwhile.

5 Summary

Measuring the impulse response of systems exhibiting nonlinear behavior by using linear systems theory is challenging. In this work, we present time-delayed mutual information (TDMI) as a potential technique for estimating the impulse response length of basic linear and nonlinear systems. From the field of information theoretics, mutual information is a nonlinear correlation metric of how much information from an output signal $y[n]$ may be caused by an input signal $x[n]$. By applying a time-delay to the input signal $x[n]$, e.g., $x[n-\tau]$, the time-delayed mutual information (TDMI) calculation measures the shared information between the delayed $x[n]$ and $y[n]$. Thus, by repeating this process over various τ, we attempt to measure the impulse response length of the underlying system $h[n]$. For sample-shifts τ where the TDMI falls below the estimator bias, we may assume that the system's impulse response $h[n]$ has fallen below the noise floor.

We validated the TDMI method by starting with simple systems such as a delay line, FIR moving-average filter, and Schroeder all-pass filters. We then investigated IIR lowpass filters to simulate encountering analog audio systems in the field. The TDMI method worked reasonably well for higher cutoff frequencies such as $f_c = 10$ and 20 kHz, but performance started to degrade as f_c was decreased down to 1kHz. Determining the cause of this phenomenon is still a work in progress. We then tried the TDMI approach after applying a static nonlinearity to the IIR lowpass filters. In most instances,

the TDMI approach tended to underreport the impulse response length compared to the linear cases.

Future work includes investigating the effect of both nonlinear distortion and decreasing f_c on the TDMI performance. Initially we thought that the TDMI suffered due to the decreased energy in $y[n]$ as f_c was lowered. However, the reason may not be so simple, as the TDMI method worked exceptionally for an all-pass filter with -120dB gain. We suspect that taking a closer look at the estimated probabilities of $x[n]$ and $y[n]$ may point to an explanation, as the TDMI calculation is inherently based on these probability calculations.

References

[1] Rife, D. D. and Vanderkooy, J., "Transfer-Function Measurement Using Maximum-Length Sequences," in *Audio Engineering Society Convention 83*, 1987.

[2] Vanderkooy, J., "Aspects of MLS Measuring Systems," *J. Audio Eng. Soc*, 42(4), pp. 219–231, 1994.

[3] Dunn, C. and Hawksford, M. J., "Distortion Immunity of MLS-Derived Impulse Response Measurements," *J. Audio Eng. Soc*, 41(5), pp. 314–335, 1993.

[4] Orcioni, S., Terenzi, A., Cecchi, S., Piazza, F., and Carini, A., "Identification of Volterra Models of Tube Audio Devices using Multiple-Variance Method," *Journal of the Audio Engineering Society*, 66(10), pp. 823–838, 2018.

[5] Cover, T. M. and Thomas, J. A., "Elements of Information Theory. Wiley Series in Telecommunications." 1991.

[6] Albers, D. J. and Hripcsak, G., "Estimation of time-delayed mutual information and bias for irregularly and sparsely sampled time-series," *Chaos, Solitons & Fractals*, 45(6), pp. 853–860, 2012, ISSN 09600779, doi:10.1016/j.chaos.2012.03.003, arXiv: 1110.1615 version: 1.

[7] Hoerr, E. and Maher, R. C., "Using Volterra Series Modeling Techniques to Classify Black-Box Audio Effects," in *Audio Engineering Society Convention 147*, 2019.

[8] Oppenheim, A. V., Schafer, R. W., and Buck, J. R., *Discrete-time Signal Processing*, Prentice-Hall signal processing series, Pearson, 2nd ed. edition, 1998, ISBN 0-18-754920-2.

[9] Smith, J. O., *Physical Audio Signal Processing*, W3K Publishing, 2010, ISBN 978-0-9745607-2-4.